ACS APPLIED MATERIALS & INTERFACES

Research Article

www.acsami.org

Engineered Coalescence by Annealing 3D Ge Microstructures into High-Quality Suspended Layers on Si

Marco Salvalaglio,[†] Roberto Bergamaschini,[†] Fabio Isa,[‡] Andrea Scaccabarozzi,[†] Giovanni Isella,[§] Rainer Backofen,[∥] Axel Voigt,[∥] Francesco Montalenti,[†] Giovanni Capellini,[⊥,#] Thomas Schroeder,[⊥] Hans von Känel,[‡] and Leo Miglio*,[†]

[†]L-NESS and Department of Materials Science, Università di Milano-Bicocca, Via R. Cozzi 55, I-20126, Milano, Italy

[‡]Laboratory for Solid State Physics, ETH Zürich, Otto-Stern-Weg 1, CH-8093, Zürich, Switzerland

[§]L-NESS and Department of Physics, Politecnico di Milano, Via F. Anzani 42, I-22100, Como, Italy

[∥]Institut für Wissenschaftliches Rechnen, Technische Universität Dresden, Zellescher Weg 12-14, D-01069, Dresden, Germany

[⊥]IHP, Im Technologiepark 25, D-15236, Frankfurt (Oder), Germany

[#]Department of Science, Università Roma Tre, Viale Marconi 446, I-00146, Roma, Italy

Supporting Information

ABSTRACT: The move from dimensional to functional scaling in microelectronics has led to renewed interest toward integration of Ge on Si. In this work, simulation-driven experiments leading to high-quality suspended Ge films on Si pillars are reported. Starting from an array of micrometric Ge crystals, the film is obtained by exploiting their temperature-driven coalescence across nanometric gaps. The merging process is simulated by means of a suitable surface-diffusion model within a phase-field approach. The successful comparison between experimental and simulated data demonstrates that the morphological evolution is driven purely by the lowering of surface-curvature gradients. This allows for fine control over the final morphology to be attained. At fixed annealing time and temperature, perfectly merged films are obtained from Ge crystals grown at low temperature (450 °C), whereas some void regions still persist for crystals grown at higher temperature (500 °C) due to their different initial morphology. The latter condition, however, looks very promising for possible applications. Indeed, scanning tunneling electron microscopy and high-resolution transmission electron microscopy analyses show that, at least during the first stages of merging, the developing film is free from threading dislocations. The present findings, thus, introduce a promising path to integrate Ge layers on Si with a low dislocation density.

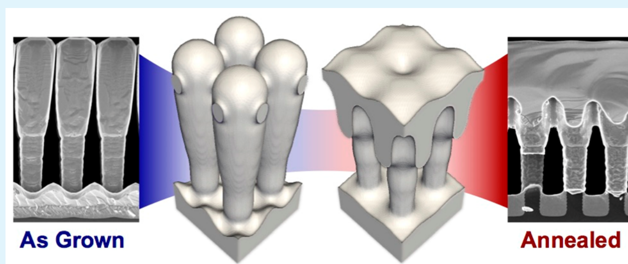

KEYWORDS: *heteroepitaxy, semiconductors, substrate patterning, surface diffusion, dislocations*

1. INTRODUCTION

Fostered by the move from dimensional to functional scaling in microelectronics,[1] germanium has been recently reinvestigated as a possible high-mobility replacement for mainstream silicon MOSFET technology.[2] However, the material growth challenges for heterogeneous integration on Si are substantial because of the 4% lattice misfit: any Ge film on Si will relax through the formation of misfit dislocations because the critical thickness for such a large misfit is only a few monolayers. To accommodate the lattice mismatch between the two materials, a thick $Si_{1-x}Ge_x$ graded layer can be grown between the silicon substrate and the active germanium layer so that the defect density is significantly reduced, but it is still not eliminated.[3] To mitigate this problem, several alternatives have been investigated, in particular, the aspect-ratio-trapping process for growing Ge and SiGe buffer layers within narrow oxide trenches, patterned on silicon substrates at submicrometer distances,[4,5] and, very recently, the use of composite AlAs/GaAs buffer layers.[6]

To date, the high-quality integration of Ge on Si beyond the nanometer scale, with no threading dislocations reaching the top part of the crystals, has been achieved only in the form of vertical, micrometer-sized Ge structures grown on deeply patterned Si substrates.[7,8] As demonstrated and discussed in refs 7, 9, and 10, full pyramidal faceting at the top regions allows for a complete lateral expulsion of threading dislocations (which are, instead, present when considering a flat top), leading to several micrometers of defect-free material. Extending such properties to a planar film would lead to substrates for microelectronic applications with unprecedented quality.

Received: June 8, 2015
Accepted: August 7, 2015
Published: August 7, 2015

ACS Publications © 2015 American Chemical Society

DOI: 10.1021/acsami.5b05054
ACS Appl. Mater. Interfaces 2015, 7, 19219−19225

In this work, we show that a perfect array of such Ge crystals can lead to the formation of a single suspended Ge layer through a lateral merging process. This is demonstrated by simulation-driven experiments, followed by extensive morphological and structural characterizations. A detailed theoretical interpretation of the merging process is also provided, and critical issues in terms of material quality are discussed.

2. EXPERIMENTAL SECTION

2.1. LEPECVD Crystal Growth and in Situ Annealing. The epitaxial growth of micrometric Ge crystals, used as starting point for the annealing process, is performed by low-energy plasma-enhanced chemical vapor deposition (LEPECVD). In this epitaxial technique, the molecules of the precursor gas, germane, are activated by low-energy (∼10 eV), magnetically confined Ar plasma, enabling the deposition of Ge crystals at a low growth temperature (400−550 °C) and high growth rate (up to 10 nm/s).[11] Prior to epitaxial growth, patterned Si substrates are treated by RCA cleaning,[12] dipped in 5% HF solution for 30 s, and rinsed in deionized water for 3 min. Afterward, the substrates are loaded into the LEPECVD load-lock, reaching a pressure of $\sim 10^{-8}$ mbar, and are finally transported into the growth chamber (base pressure of 1×10^{-9} mbar) and heated to 300 °C for 15 min before reaching the growth temperature.

In particular, the different samples considered here consist of 8 μm tall Ge crystals grown by LEPECVD at 450 or 500 °C ± 15 °C, at a rate of 4.2 nm/s and with a chamber pressure of 3×10^{-2} mbar. After epitaxial growth, an annealing treatment is performed in situ in the growth chamber (pressure of 5×10^{-7} mbar), heating the sample to 800 °C (the highest attainable annealing temperature allowed in our apparatus), at a rate of 2 °C/s. The annealing time is measured starting when the sample reaches 800 ± 10 °C. Thermal cycles are also performed in some cases by repeatedly varying the temperature between 600 and 800 °C with a heating ramp of 1 °C/s and cooling at 2 °C/s.

2.2. Morphology Analysis. The morphology of the as-grown and annealed Ge crystals is investigated by means of atomic force microscopy (AFM) using an Asylum Research MFP-3D and scanning electron microscopy (SEM) using a Zeiss ULTRA 55 digital field emission apparatus. The density of threading dislocations in the Ge crystals and in the planar unpatterned area is inferred by selective defect etching and etch-pit counting by means of AFM, SEM, and Nomarski microscopy (Nikon Eclipse 200D) on an area of at least 500 × 500 μm^2. The etching procedure consists of dipping the Ge samples into an iodine-based solution (15 mg of I_2, 33 mL of glacial acetic acid, 10 mL of 65% nitric acid, 5 mL of 40% HF) for 40 s at 0 °C.[13] The quality of the merged region is assessed by scanning tunneling electron microscopy (STEM) and high-resolution transmission electron microscopy (HR-TEM) using a FEI Tecnai Osiris system.

2.3. Phase-Field Simulations. The process of adjacent Ge crystals merging is investigated by means of numerical simulations based on a phase-field approach (see ref 14 for a review), which permits three-dimensional (3D) domains to be easily managed and naturally accounts for complex topological changes. The surface profile is implicitly tracked by means of an order parameter φ varying continuously from 1 inside the solid to 0 outside, as given by $\varphi(\mathbf{x}) = 0.5[1 - \tanh(3d(\mathbf{x})/\varepsilon)]$, where ε is the interface width and d is the signed distance from the profile of the surface, located at $\varphi = 0.5$. In Figure 1a, the $\varphi = 0.5$ isosurface corresponding to a Ge crystal is shown. According to the Onsager linear law, material transport is described by $\partial\varphi/\partial t = \nabla\cdot[M(\varphi,\mathbf{x})\gamma\nabla\kappa]$, where $\kappa = \kappa(\varphi(\mathbf{x}))$ accounts for the local curvature of the surface and γ is the surface energy density, here assumed to be isotropic because faceting is not found to play a crucial role (see Supporting Information, where surface anisotropy is tackled by exploiting the method introduced in ref 15). Finally, M is the mobility function, restricted to the surface by the typical setting $M = M_0(36/\varepsilon)\varphi^2(1 - \varphi)^2$, where M_0 is a scaling factor, forced to be zero inside the Si region ($M_0 \sim 0$; see Figure 1b) in order to account for the stability of the Si pillars at the annealing temperatures[16] (SiGe intermixing is not considered). The isotropic surface energy γ is

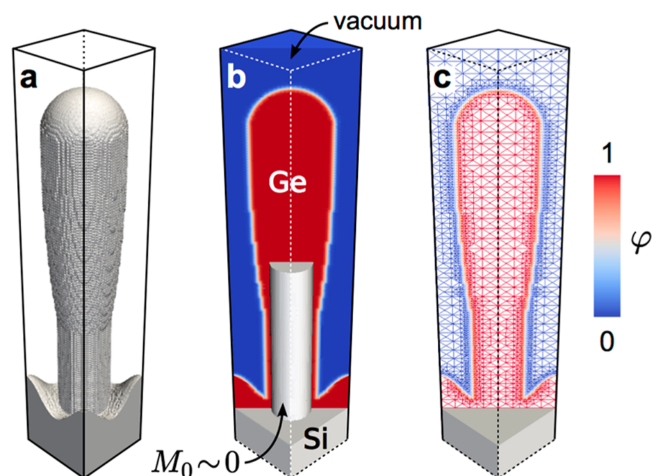

Figure 1. Phase-field modeling. (a) 3D view of the simulation cell embedding a pillar-like structure implicitly defined according to the phase-field approach. The profile corresponds to the isosurface at φ = 0.5. (b) Cross-section of the cell showing the variation of φ from the solid region to vacuum. The 3D gray region corresponds to the immobile Si pillar ($M_0 \sim 0$). (c) Mesh structure with local refinement at the surface of the solid phase, i.e., at φ = 0.5. The color map reports the values of φ.

chosen to be unitary, so the simulation time scale is directly determined by M_0 only. Numerical simulations are performed by using the finite element method toolbox AMDiS.[17,18] Local mesh refinement is adopted in order to improve the spatial resolution in the region where φ = 0.5, i.e., at the surface of the solid phase (Figure 1c). This space adaptivity allows the details of the surface to be accurately defined while minimizing the computational cost. A semi-implicit integration scheme is implemented. The boundary conditions are set to be periodic in the [110] and [$1\bar{1}0$] directions, whereas zero-flux Neumann boundaries are imposed in the [001] direction, i.e., at the top and bottom of the simulation cell. Both sequential and parallel executions are considered with direct and iterative solvers. Further details are reported in the Supporting Information.

3. RESULTS AND DISCUSSION

3.1. Morphological Evolution. As illustrated in refs 7 and 8, the epitaxial growth of Ge onto an array of micrometers-tall Si pillars in a highly kinetic regime may result in closely spaced individual Ge crystals, separated by gaps as large as tens of nanometers. This particular 3D morphology results from the combined effect of a short diffusion length, ensured by the high deposition rate (∼4 nm/s) of LEPECVD at comparatively low temperatures (∼450−500 °C), and mutual shielding of the reactive gas flux by neighboring crystals. A typical pattern consists of 8 μm tall Si pillars spaced by a few micrometers, as shown in Figure 2a, for the specific case of 2 × 2 μm^2 Si pillars with 2 μm trenches. A perspective SEM view of an as-grown 8 μm tall Ge crystal on top of a 2 × 2 μm^2 Si pillar is shown in Figure 2b. The crystal is bounded by {110} sidewalls and {113} and {111} top facets, typical at the growth temperature of 500 °C and for the present Si pillar size. An additional (001) surface facet is usually found on crystals grown at lower temperature or on larger Si pillars[8] (see below). This morphological feature is important since only as-grown crystals with fully slanted facets at the growth front were shown to be free of threading dislocations[7,9,10] without the need for postgrowth annealing, which is usually performed on planar substrates to improve the crystal's quality. However, the morphology of these Ge crystals does change upon annealing, as indicated in the SEM and AFM

DOI: 10.1021/acsami.5b05054
ACS Appl. Mater. Interfaces 2015, 7, 19219−19225

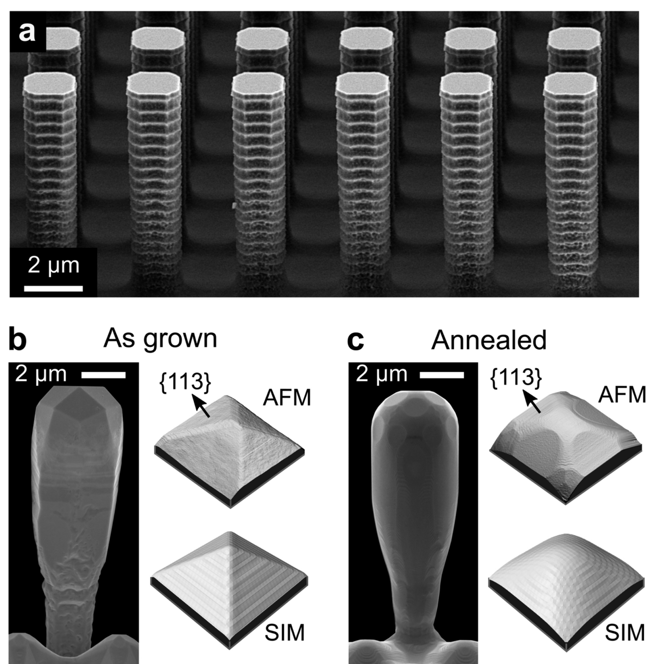

Figure 2. Growth and annealing of individual crystals. (a) SEM lateral view of a pattern formed by 2 × 2 μm^2 wide Si pillars with a 2 μm trench prior to deposition. SEM lateral views and AFM perspective views of the Ge crystal are shown for: (b) as-grown 8 μm tall Ge crystal obtained by deposition at 500 °C on a Si substrate patterned with 8 μm tall and 2 × 2 μm^2 wide pillars, spaced by 3 μm trenches; (c) in situ annealing of the structure in panel (b) by six thermal cycles ranging from 600 to 800 °C. The top morphology in (c) is compared with the profile resulting from a phase-field simulation (SIM) of surface diffusion starting from the as-grown geometry, as sketched in the inset of panel (b).

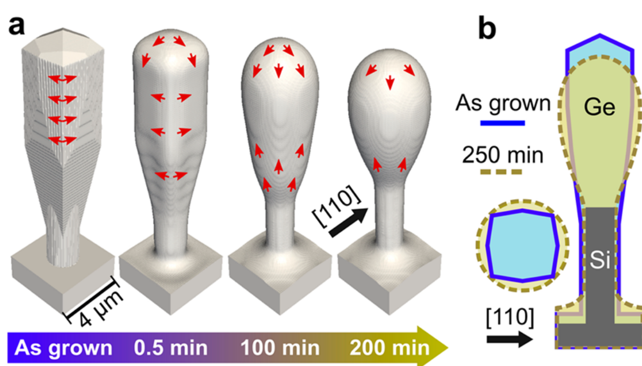

Figure 3. Simulation of annealing of an isolated crystal. (a) Phase-field simulation of the profile evolution of an isolated crystal, starting from the as-grown geometry shown in Figure 2b. Illustrative arrows show the material fluxes given by the local curvature. (b) Cross- and top-view comparison between the first and the last simulation stages in panel (a).

images of Figure 2c. These images were obtained after six thermal cycles between 600 and 800 °C, each one lasting for 6 min. Evidently, the annealing causes smoothening of the edges between the {113} facets and flattening of the top cusp toward a (001) facet, indicating that the morphology is beginning to evolve toward equilibrium. In the absence of deposition, the changes in the profile must be attributed to material redistribution driven by the tendency of the system to minimize its free energy. Since the Ge crystals are strain-free,[7,9,10] the morphological changes must be driven by surface energy lowering. Bulk diffusion can be excluded at the annealing temperatures in view of its high activation barrier.[19]

On the basis of these considerations, we have developed a 3D surface diffusion model, where the chemical potentials are derived by the local curvature,[20] implemented in a suitable phase-field framework in order to describe the morphological evolution during the annealing process. Details of the model are provided in the Experimental Section and Supporting Information. We did not include any facet-dependent surface energy, in order to simplify the model, with no loss of predictive power (as demonstrated in the Supporting Information). Since the average mobility M_0 of Ge along the surface profile cannot be predicted by calculations, we use it as a free parameter to quantitatively match the experimental time scale. Annealing simulations based on this description are quite effective in capturing the initial edge smoothening at the top of the Ge crystal, as reported in the lower inset of Figure 2c. By extending the simulations to much longer annealing times, a global rounding of the Ge crystal profile is obtained, with significant lateral expansion. This is illustrated in Figure 3a, where snapshots of a prolonged annealing simulation are reported. The morphological change can be interpreted as being caused by significant material fluxes from the top and the vertical edges to the center of the sidewalls (as indicated by red arrows) in order to equilibrate the local surface curvature, which, in turn, determines the chemical potential. To better appreciate the extent of such a process, cross-section and top views of the crystals are compared for the initial and final stages of the simulation in Figure 3b.

As already mentioned, adjacent Ge crystals grown under such conditions on Si pillars spaced 2 μm are separated by gaps of just a few dozen nanometers.[7,8] Therefore, we expect that, for sufficiently long postgrowth annealing times, neighboring Ge crystals will touch in the upper part and gradually merge, eventually resulting in a flat suspended Ge layer on top of the Si pillars. In order to verify this assumption, in situ annealing experiments were performed at increasing times up to 60 min at 800 °C. Figure 4 illustrates the morphology evolution of 8 μm tall Ge crystals on top of 8 μm Si pillars. Top (a) and lateral (b) SEM images as well as AFM perspective views (c−f) of the crystal tops are reported for different durations of the annealing process (additional data are provided in Figure S1 in the Supporting Information). The initial individual crystals obtained after the LEPECVD growth at 450 °C on 2 × 2 μm^2 Si pillars spaced by 2 μm exhibit a top (001) facet and are spaced ∼150 nm apart. Similar to the isolated structures of Figure 2, the crystals assume a rounded shape after an annealing time of 5 min (Figure 4a). Some of them are already touching at this stage and eventually merge along the ⟨110⟩ directions (10 and 20 min), whereas sizable undulations at the top remain along with a regular array of holes at the crossing of the original Si trenches. It is evident from the enlarged AFM scan of a single Ge crystal annealed for 10 min, reported in Figure 4d, that the original facets have blurred to an almost continuous smooth profile with a large density of surface steps, probably resulting in a slowing of the surface mobility. Finally, after an annealing time of 60 min, the holes are closed and a continuous film is obtained (see Figures 4). The AFM scans indicate a peak-to-valley amplitude of about 250 nm, still phase-matched to the underlying pattern of Si pillars.

In order to obtain deeper insight into the diffusion mechanisms leading to the observed morphological changes,

DOI: 10.1021/acsami.5b05054
ACS Appl. Mater. Interfaces 2015, 7, 19219−19225

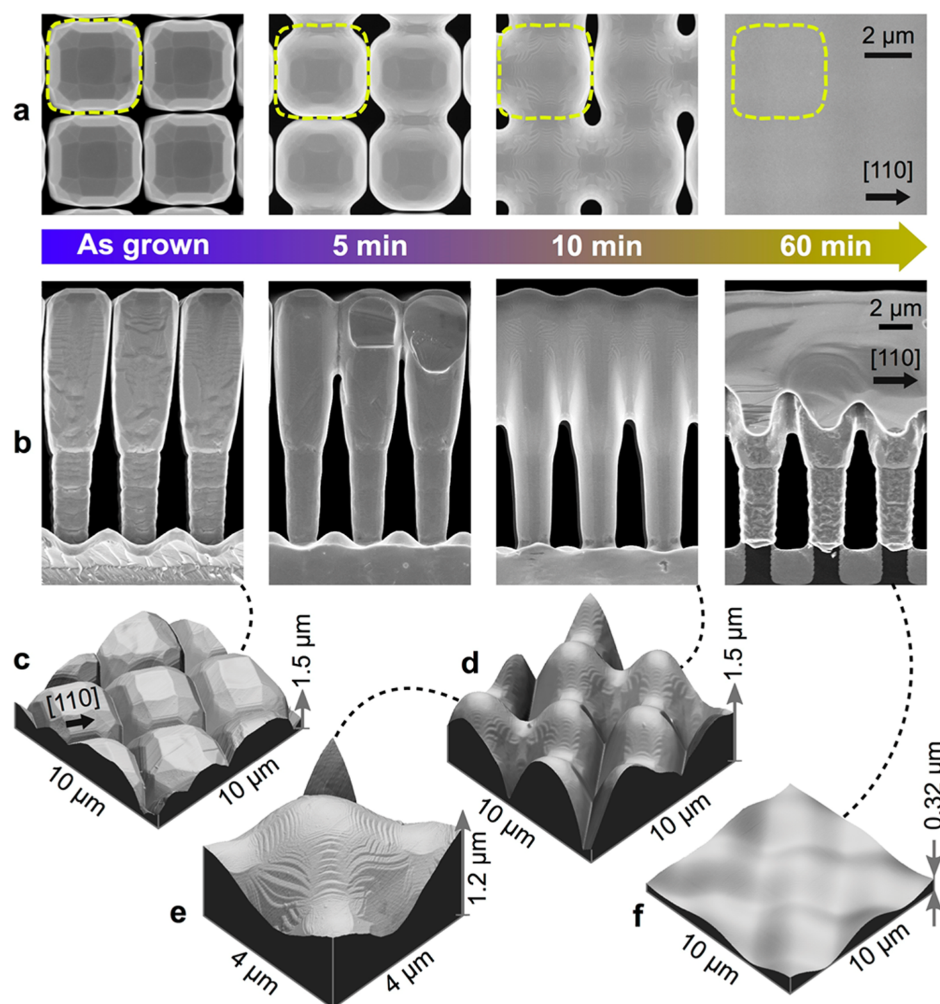

Figure 4. Coalescence process induced by annealing. (a) Top and (b) lateral SEM views of Ge crystals grown at 450 °C on 8 μm tall and 2×2 μm^2 wide Si pillars separated by 2 μm trenches after in situ annealing experiments of different durations at 800 °C. AFM views of the samples reported in panels (a) and (b) are shown: (c) as-grown and (d) after annealing for 10 min; (e) magnification of the top of a fused crystal in (d), revealing the existence of stepped regions along the facets, and (f) after annealing for 60 min.

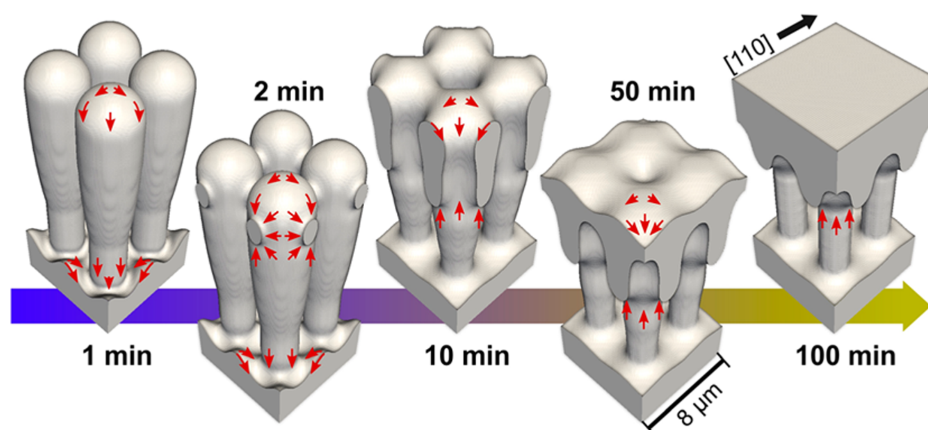

Figure 5. Phase-field simulations of the coalescence process. Snapshots of the phase-field simulation matching the main features of the annealing experiments shown in Figure 4 (a movie showing the whole evolution is provided in the Supporting Information).

simulations for dense arrays are performed, with the same geometric parameters as those used for the experimental case of Figure 4 but, with no loss of generality, for the slightly rounded initial shape indicated in Figure 2c. Figure 5 shows that the initial lateral expansion due to thermal treatment of crystals quickly reduces their distance so that they touch. At the onset of merging, here corresponding to an annealing time of $t = 2$ min, the contact region has an almost circular cross-section and acts as a collector for neighboring material due to differences in the local curvature (see Figure S2 in the Supporting

DOI: 10.1021/acsami.5b05054
ACS Appl. Mater. Interfaces 2015, 7, 19219−19225

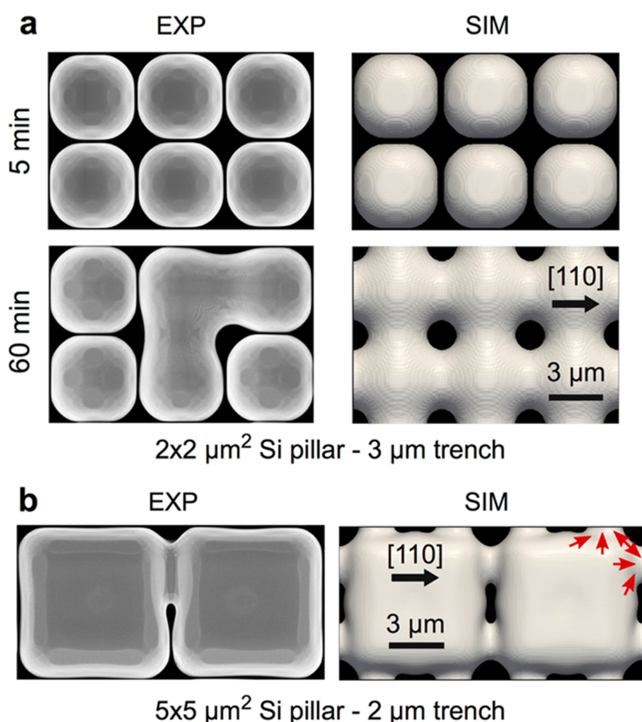

Figure 6. Features of the coalescence process. (a) SEM (left, EXP) and simulation (right, SIM) top views of samples obtained after annealing for 5 and 60 min of 8 μm tall Ge crystals grown at 450 °C on 8 μm tall and 2×2 μm^2 wide Si pillars spaced by 3 μm trenches. (b) SEM (left) and simulation (right) top views of samples obtained after annealing for 5 min of 8 μm tall Ge crystals grown at 450 °C on 8 μm tall and 5×5 μm^2 large Si pillars spaced by 2 μm trenches. Illustrative arrows in panel (b) show the material fluxes in a representative region.

Information). The expansion of these regions allows the system to reduce its surface energy. Simultaneously, Ge material originating from the lower part of the sidewalls is found to move upward in a kind of a zipping action, further closing the trenches between the crystals. A thick suspended film with holes located at the crossings of the trenches is then formed (t = 10 min). At this stage, the structure is, however, not yet in equilibrium, as the holes provide a gradient in the local curvatures so that Ge is collected from both the top and bottom of the crystals until the holes are completely closed. This leaves an undulated surface profile of the resulting film at t = 50 min, which slowly flattens until t = 100 min. This prediction nicely agrees with the experimental behavior observed in Figure 4 (see also the movie in the Supporting Information). We therefore conclude that the surface curvature is the main driving force leading to the coalescence of the crystals.

Such a mechanism is valid in general, provided that the crystal aspect ratio is sufficiently large that the initial lateral expansion causes a bridging of the gaps somewhere. In order to prove this, we considered different patterns, both in experiments and simulations. In Figure 6a, we show the annealing results, after 5 and 60 min, of 8 μm tall Ge crystals grown on a pattern of 2×2 μm^2 Si pillars separated by 3 μm wide trenches, leading to a distance of ~300 nm in their as-grown state. Due to the larger gap, the lateral expansion after an annealing time of 5 min is not sufficient to create a bridge. Instead, only rounding of the crystals is observed, both in experiments and simulations. Only upon extending the annealing time to 60 min, it is possible to see the onset of crystal merging. This delay in the uniform coalescence is observed also in the simulations, although it is not as long. Possibly, the slower experimental evolution is due to the dense step bunching already seen in the AFM scan of Figure 4e. The effect of a different lateral size of the Si pillars is, instead, shown in Figure 6b (see also Figures S3−S5 in the Supporting Information). Here, 5×5 μm^2 Si pillars are seen to lead to the formation of Ge crystals with a much wider (001) top facet of nearly square shape. The top SEM view of Figure 6b applies to samples characterized by 2 μm wide Si trenches and annealed for 5 min. Again, the simulation matches the SEM profiles, revealing that bridging in this case takes place close to the corners of the Ge crystals. This happens because the four top edges are smeared out, producing enough accumulation of material at their sides (see red arrows and Figure S5 in the Supporting Information) to initiate coalescence.

3.2. Material Quality. So far, the very good agreement between the simulated and experimental evolution toward full

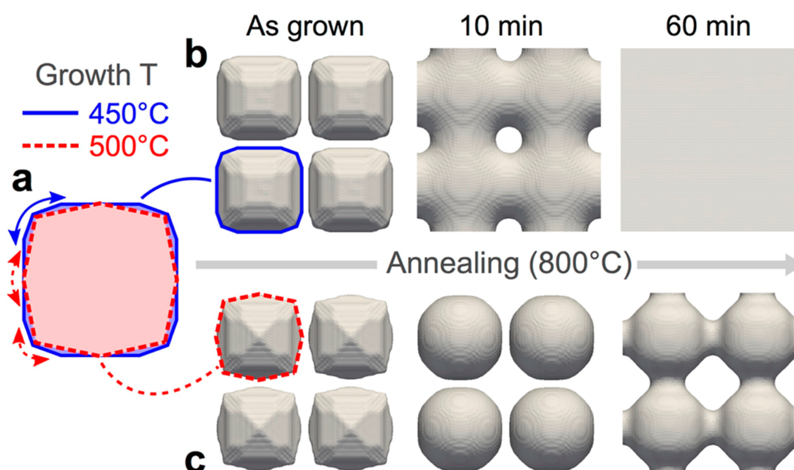

Figure 7. Influence of the as-grown morphology. (a) Comparison between the top sections of Ge crystals grown at 450 °C (solid blue line) and 500 °C (dashed red line). (b, c) Simulation results of the evolution driven by surface diffusion resulting from the two different initial top morphologies in panel (a). The same mobility coefficient M_0 used in the simulation of Figure 6 is considered for both cases (b, c). In agreement with experiments, the coalescence process is delayed for the structure grown at high temperature (b).

DOI: 10.1021/acsami.5b05054
ACS Appl. Mater. Interfaces 2015, 7, 19219−19225

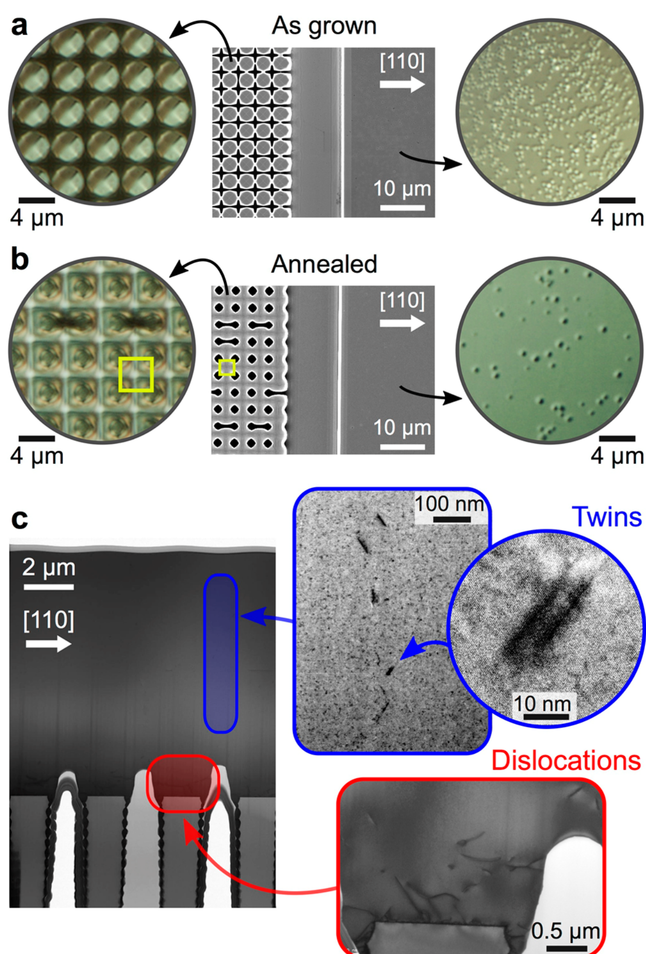

Figure 8. Quality of the coalesced structure. (a, b) Etch-pit analysis shown by SEM and Nomarski microscopy (circular enlarged views). Both planar unpatterned and patterned regions, the latter corresponding to 2×2 μm^2 wide 8 μm tall Si pillars spaced by 2 μm trenches, are considered. Samples obtained by 8 μm Ge deposition at 500 °C are shown before (a) and after (b) in situ annealing by six thermal cycles as reported in Figure 2. (c) STEM bright-field cross-section of the sample in panel (b). Insets show magnifications of both twins and dislocations obtained by bright-field HR-TEM.

coalescence may be considered to be of mere fundamental interest. Indeed, the suspended film discussed above resulted from the merging of crystals characterized by extended, flat (001) top facets. As mentioned in the Introduction, this leads to a nonvanishing threading-dislocation density in the top region.[10] Our final goal, however, is to provide a path leading to virtually dislocation-free suspended Ge films on Si. To this end, it is necessary to form the coalesced film from a set of Ge pillars featuring fully pyramidal top faceting, as found for narrow Si pillars and the higher growth temperature shown in Figure 2. In refs 7, 9, and 10, we indeed demonstrated that no threading dislocations are present in the upper part of the crystals, where the merging induced by annealing begins. Any additional dislocations nucleating during coalescence would have to reside, therefore, in a cylindrical expanding bridge, which is still surrounded by free surfaces. These free surfaces may be expected, however, to gather nucleated defects. As the fully faceted top profile is closer to a rounded shape (see Figure 7a), with smaller curvature gradients, the annealing time for full coalescence is expected to be larger than in the case of more squared profiles (found for larger Si pillars or lower growth temperatures). This is actually confirmed by the simulations reported in Figure 7b,c. From the reported comparison at fixed annealing time and temperature between the evolution of an array of Ge crystals grown at 450 °C (flat top) and 500 °C (pyramidal, fully faceted top), indeed, it can be seen that coalescence does take place in both cases, but merging is far from completed when starting from a pyramidal shape even after the maximum annealing time (60 min) at the maximum temperature (800 °C) available in our growth chamber. This was indeed confirmed by experiments, as demonstrated in Figure 8 (center of panel (b)). The following dislocation analysis is limited, therefore, to a connected network including the expanded cylindrical bridges with a periodic array of small holes rather than a fully coalesced film. In Figure 8a,b, we report the results of an etch-pit analysis by Nomarski interference microscopy (circular enlarged views) after selective defect etching (see Experimental Section) on as-grown and 60 min annealed Ge samples. These images are combined with top-view SEM images, showing the patterned region close to the planar region. We see that etch-pits related to emerging threading dislocations are present in the planar region of the as-grown sample (density of $(3 \pm 1) \times 10^8$ cm^{-2}), whereas no etch-pits were found in an area of 30×30 Ge crystals (corresponding to a maximum dislocation density of 7×10^4 cm^{-2}). After thermal annealing, the etch-pit density in the planar region is lowered by a factor of ~30, whereas no additional etch-pits appear upon crystal merging in the patterned region of the same size as that in the as-grown case. This statistically relevant information is supported also by STEM and HR-TEM cross-section views, taken along a cut in the [110] direction, passing through the centers of the coalescence bridges, as reported in Figure 8c. Here, we see that dislocations are indeed present close to the bottom of the Ge crystals, whereas only twin defects are seen in a columnar distribution in the bridge region. Indeed, small angle grain boundaries must be expected to originate from the small random Ge crystal tilts, analyzed in-depth in ref 9. These results show the superior potential of the present technique with respect to other coalescence methods widely exploited in group IV or III−V semiconductors, such as epitaxial lateral overgrowth (ELO),[21−24] which lead to defected merging regions.

4. CONCLUSIONS

We have demonstrated that a flat, thick suspended Ge layer can be obtained from an array of isolated Ge crystals by exploiting the surface diffusion of material during annealing. A surface-diffusion model based on a phase-field approach was used first to guide experiments and then to give an interpretation of the findings. The good agreement between experimental and simulated morphologies allowed the full merging process to be attributed to a single, dominating driving force: surface curvature.

Further optimization in the growth/annealing procedure is still needed in order to obtain continuously flat suspended layers starting from crystals free of any threading dislocation at their tops. Unfortunately, extending the annealing time to a few hours and/or increasing the temperature were not possible in our growth chamber, but our simulations indicate that a flat film is eventually obtained. Ex situ annealing is also viable, provided that complete Ge oxide removal is performed and that thermal treatment in a suitable atmosphere is operated to maintain high Ge mobility, which is still not possible in our

DOI: 10.1021/acsami.5b05054
ACS Appl. Mater. Interfaces 2015, 7, 19219−19225

laboratory. However, characterization of partially coalesced films already indicates a promising path to produce suspended Ge layers with low dislocation density by controlling the merging across engineered nanometric gaps.

Importantly, similar results can be achieved with vertical crystals obtained by growth techniques other than LEPECVD, provided that surface diffusion lengths can be kept on a submicrometer scale. Finally, preliminary tests indicate that the same merging process can be applied also to Ge-rich $Si_{1-x}Ge_x$ crystals[8] to be subsequently topped by a thin Ge layer; the method may also become suitable for the monolithic integration of strained Ge MOSFETs on silicon substrates, the next target of the present technology roadmap of microelectronics.

■ ASSOCIATED CONTENT

Supporting Information

The Supporting Information is available free of charge on the ACS Publications website at DOI: 10.1021/acsami.5b05054.

Full video reporting the evolution shown in Figure 5 (MPG).

Further details on phase-field modeling and on the coalescence process, the detailed evolution of large crystals, and the role of the anisotropic surface-energy density in the simulated evolutions (PDF).

■ AUTHOR INFORMATION

Corresponding Author

*E-mail: leo.miglio@unimib.it.

Notes

The authors declare no competing financial interest.

■ ACKNOWLEDGMENTS

We are grateful to M. A. Schubert (IHP Frankfurt Oder) for technical support in the STEM analysis, to P. Niedermann (CSEM Neuchâtel) for providing the patterned substrates and C. V. Falub (Evatec AG) for taking the image in Figure 2a, to D. Chrastina (L-NESS, Politecnico di Milano) for accurately revising the manuscript, and to A. Marzegalli (Università di Milano-Bicocca) for helpful discussions on dislocations. We gratefully acknowledge support of Pilegrowth Tech S.r.l. and of the Project NOVIPIX CRSII2_147639 of the Swiss National Science Foundation.

■ REFERENCES

(1) Dai, X.; Nguyen, B.-M.; Hwang, Y.; Soci, C.; Dayeh, S. A. Novel Heterogeneous Integration Technology of III−V Layers and InGaAs FinFETs to Silicon. *Adv. Funct. Mater.* **2014**, *24*, 4420−4426.

(2) Pillarisetty, R. Academic and Industry Research Progress in Germanium Nanodevices. *Nature* **2011**, *479*, 324−328.

(3) Currie, M. T.; Samavedam, S. B.; Langdo, T. A.; Leitz, C. W.; Fitzgerald, E. A. Controlling Threading Dislocation Densities in Ge on Si Using Graded SiGe Layers and Chemical-Mechanical Polishing. *Appl. Phys. Lett.* **1998**, *72*, 1718−1720.

(4) Park, J.-S.; Bai, J.; Curtin, M.; Adekore, B.; Carroll, M.; Lochtefeld, A. Defect Reduction of Selective Ge Epitaxy in Trenches on Si(001) Substrates Using Aspect Ratio Trapping. *Appl. Phys. Lett.* **2007**, *90*, 052113.

(5) Wang, G.; Rosseel, E.; Loo, R.; Favia, P.; Bender, H.; Caymax, M.; Heyns, M. M.; Vandervorst, W. High Quality Ge Epitaxial Layers in Narrow Channels on Si (001) Substrates. *Appl. Phys. Lett.* **2010**, *96*, 111903.

(6) Hudait, M. K.; Clavel, M.; Goley, P.; Jain, N.; Zhu, Y. Heterogeneous Integration of Epitaxial Ge on Si using AlAs/GaAs Buffer Architecture: Suitability for Low-Power Fin Field-Effect Transistors. *Sci. Rep.* **2014**, *4*, 6964.

(7) Falub, C. V.; von Känel, H.; Isa, F.; Bergamaschini, R.; Marzegalli, A.; Chrastina, D.; Isella, G.; Müller, E.; Niedermann, P.; Miglio, L. Scaling Hetero-Epitaxy from Layers to Three-Dimensional Crystals. *Science* **2012**, *335*, 1330−1334.

(8) Bergamaschini, R.; Isa, F.; Falub, C. V.; Niedermann, P.; Müller, E.; Isella, G.; von Känel, H.; Miglio, L. Self-Aligned Ge and SiGe Three-Dimensional Epitaxy on Dense Si Pillar Arrays. *Surf. Sci. Rep.* **2013**, *68*, 390−417.

(9) Falub, C. V.; Meduňa, M.; Chrastina, D.; Isa, F.; Marzegalli, A.; Kreiliger, T.; Taboada, A. G.; Isella, G.; Miglio, L.; Dommann, A.; von Känel, H. Perfect Crystals Grown from Imperfect Interfaces. *Sci. Rep.* **2013**, *3*, 2276.

(10) Marzegalli, A.; Isa, F.; Groiss, H.; Müller, E.; Falub, C. V.; Taboada, A. G.; Niedermann, P.; Isella, G.; Schäffler, F.; Montalenti, F.; von Känel, H.; Miglio, L. Unexpected Dominance of Vertical Dislocations in High-Misfit Ge/Si(001) Films and Their Elimination by Deep Substrate Patterning. *Adv. Mater.* **2013**, *25*, 4408−4412.

(11) Rosenblad, C.; Deller, H. R.; Dommann, A.; Meyer, T.; Schroeter, P.; von Känel, H. Silicon Epitaxy by Low-Energy Plasma Enhanced Chemical Vapor Deposition. *J. Vac. Sci. Technol., A* **1998**, *16*, 2785−2790.

(12) Kern, W.; Puotinen, D. A. Cleaning Solutions Based on Hydrogen Peroxide for Use in Silicon Semiconductor Technology. *RCA Rev.* **1970**, *31*, 187−206.

(13) Marchionna, S.; Virtuani, A.; Acciarri, M.; Isella, G.; von Känel, H. Defect Imaging of SiGe Strain Relaxed Buffers Grown by LEPECVD. *Mater. Sci. Semicond. Process.* **2006**, *9*, 802−805.

(14) Li, B.; Lowengrub, J.; Ratz, A.; Voigt, A. Geometric Evolution Laws for Thin Crystalline Films: Modeling and Numerics. *Comm. Comput. Phys.* **2009**, *6*, 433−482.

(15) Salvalaglio, M.; Backofen, R.; Bergamaschini, R.; Montalenti, F.; Voigt, A. Faceting of Equilibrium and Metastable Nanostructures: A Phase-Field Model of Surface Diffusion Tackling Realistic Shapes. *Cryst. Growth Des.* **2015**, *15*, 2787−2794.

(16) Huang, L.; Liu, F.; Lu, G.-H.; Gong, X. G. Surface Mobility Difference between Si and Ge and Its Effect on Growth of SiGe Alloy Films and Islands. *Phys. Rev. Lett.* **2006**, *96*, 016103.

(17) Vey, S.; Voigt, A. AMDiS: Adaptive Multidimensional Simulations. *Comput. Visualization Sci.* **2007**, *10*, 57−67.

(18) Witkowski, T.; Ling, S.; Praetorius, S.; Voigt, A. Software Concepts and Numerical Algorithms for a Scalable Adaprive Parallel Finite Element Method. *Advances in Computational Mathematics* **2015**, DOI: 10.1007/s10444-015-9405-4.

(19) Uberuaga, B. P.; Leskovar, M.; Smith, A. P.; Jonsson, H.; Olmstead, M. Diffusion of Ge below Si(100) Surface: Theory and Experiment. *Phys. Rev. Lett.* **2000**, *84*, 2441−2444.

(20) Mullins, W. W. Theory of Thermal Grooving. *J. Appl. Phys.* **1957**, *28*, 333−339.

(21) Gupta, A.; Jacob, C. Selective Epitaxy and Lateral Overgrowth of 3C-SiC on Si − A review. *Prog. Cryst. Growth Charact. Mater.* **2005**, *51*, 43−69.

(22) Kim, S. W.; Cho, Y. D.; Park, W. K.; Kim, D. H.; Ko, D. H. Defect Analyses of Selective Epitaxial Grown GaAs on STI Patterned (001) Si Substrates. *J. Cryst. Growth* **2014**, *401*, 319−322.

(23) Kim, B.; Kim, S.-W.; Jang, H.; Kim, J.-H.; Koo, S.; Kim, D.-H; Min, B.-G.; Park, S.-J.; Song, J. S.; Ko, D.-H. Strain Evolution during the Growth of Epitaxial Ge Layers between Narrow Oxide Trenches. *J. Cryst. Growth* **2014**, *401*, 308−313.

(24) Leonhardt, D.; Sheng, J.; Cederberg, J. G.; Qiming, L.; Carrol, M. S.; Sang, M. H. Nanoscale Interfacial Engineering To Grow Ge on Si as Virtual Substrates and Subsequent Integration of GaAs. *Thin Solid Films* **2010**, *518*, 5920−5927.

DOI: 10.1021/acsami.5b05054
ACS Appl. Mater. Interfaces 2015, 7, 19219−19225